AIAA'87

AIAA-87-1054

Lunar Capture Orbits, a Method of Constructing Earth Moon Trajectories and the Lunar Gas Mission

E.A. Belbruno
Jet Propulsion Laboratory
Pasadena, California

This is the first paper on the discov. of ballistic capture transfers and fuzzy boundary

Proceedings of the

19th AIAA/DGLR/JSASS International Electric Propulsion Conference

May 11-13, 1987/Colorado Springs, Colorado

LUNAR CAPTURE ORBITS, A METHOD OF CONSTRUCTING EARTH MOON TRAJECTORIES AND THE LUNAR GAS MISSION

E. A. Belbruno*
Jet Propulsion Laboratory
California Institute of Technology
Pasadena, California 91109

Abstract

A method is described to construct trajectories from the Earth to the Moon which utilizes the existence of Lunar capture orbits and the concept of 'stability boundary'. These orbits are ballistic and represent a new family of trajectories. They go into orbit about the Moon from a suitable position about the Earth with no required thrusting. This method is applied to a mission being studied at JPL called Lunar GAS (Get Away Special). Other applications are discussed.

1. Introduction

We describe a method of constructing trajectories from the Earth to the Moon which are ballistically captured. That is, they go into orbit about the Moon with no required thrusting. The amount of time they stay in orbit about the Moon depends on their relative stability. In general, they will orbit the Moon for several cycles and then leave the Moon's vicinity. These Lunar capture orbits start from a point P about the Earth and go to a desired point Q about the Moon. The precise position of P and the necessary velocity there must be determined in order to reach Q. In order for the orbit at Q to be ballistically captured, Q must be at a critical position from the Moon which is dependent on the approach direction. At this position, the gravitational forces of the Earth and Moon tend to cancel. Thus, the orbit can be pulled into the Moon's dynamic influence with negligible force. In general, there is a complex region about the Moon that Q belongs to where the gravitational forces of the Earth and Moon tend to balance. We call this the 'stability boundary'. A more precise formulation of the stability boundary is given in Section 2 and in the Appendix. For brevity, this is only briefly presented. The approach taken for the construction of Lunar capture orbits uses concepts from the fields of dynamical systems and stability theory of Hamiltonian systems[1,2]. This is because of the delicate nature of these orbits which is partially addressed by results in these fields.[2,5,9] The inclusion of thrusting along these orbits in order to achieve capture conditions is not covered in this paper. In this case, optimization techniques may be useful. A Newton's algorithm is derived in the Appendix which will yield the conditions at P necessary in order to achieve capture conditions at Q given the desired approach direction.

*Member of Technical Staff

Lunar capture orbits are well suited for applications to S/C with low thrust. If the thrust level is low, then it is desirable to approach the Moon in such way so as to minimize the force necessary in order to put the S/C into Lunar orbit. A Lunar capture orbit will be an ideal case since no thrusting force at all is required. In reality, of course, this ideal case will not be realized, but something close should be.

In applications, it is desirable to construct Earth Moon trajectories from low Earth orbit to low Lunar orbit. If we assume low thrust, then the S/C will slowly spiral outwards and eventually reach the point P. The rate of the spiral radial increase depends on the thrusting regime. The thrust can in general be adjusted to achieve the necessary velocity at P to match the initial capture orbit conditions. When the S/C reaches Q, the thrusting can be resumed in order to spiral down to low Lunar orbit. The complete Earth Moon trajectory can therefore be viewed in three parts: The Earth spiral phase to P, the Lunar capture orbit, or linking orbit, from P to Q, and the Lunar spiral phase from Q to low Lunar orbit. This is illustrated in Figure 1. In this figure the S/C is captured at Q above the north Lunar pole. This will be compatible with the requirements for the Lunar Gas mission.

The orbit construction above is applied to the Lunar Gas mission being studied at JPL.[11] Because this mission is described in (11), we describe it only briefly. The Lunar GAS S/C is designed to be ejected from a Get Away Special cannister aboard the shuttle from a low Earth orbit at about 300 km altitude. Upon ejection, the solar panels are extended. The S/C uses solar electric ion propulsion where the ionizing gas is Xenon. The thrust

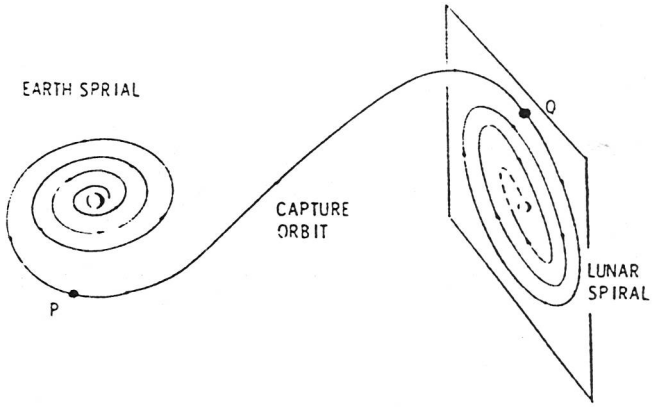

Figure 1. Earth Moon Trajectory

is initially about .04 Newtons, and the mass flow rate is 9.59×10^{-7} kg/s. The S/C has a mass of approximately 150 kg. The S/C is spin stabilized, and spins perpendicular to the thrust direction. As is shown in Figure 2, in the outgoing Earth spiral the thrust vector is first in the anti-Sun direction, and in the orbit plane. The thrust remains on for a 90° arc which is centered at the

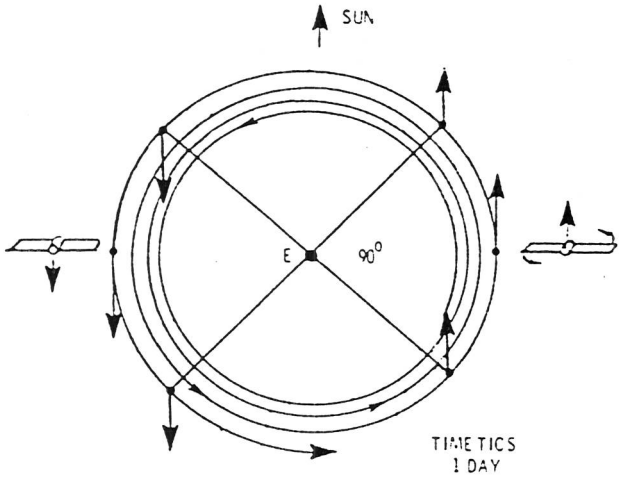

Figure 2. Earth Spiral Thrusting

point on the spiral arc where the tangent vector is parallel to the projection of the Sun direction on the orbit plane. At the end of this arc the thrust stops, and the S/C coasts for 90°. It then resumes thrusting in the Sun direction for another 90° arc at the end of which it coasts for 90°, etc. By thrusting in this fashion, the S/C performs several thousand spirals where it eventually reaches a critical position P in about 2 years. The point P is about 200,000 km from the Earth. The thrust is adjusted so that at P the velocity matches the initial condition for the Lunar capture orbit to Q over the north Lunar pole. The capture orbit has a duration of about 16 days. If no thrusting were done at Q, the capture orbit would go into orbit about the Moon, which will, in general, be unstable as indicated above. However, a relatively stable permanent capture may be possible. In order to stabilize it, the thrusting can be resumed in a way analogous to the Earth spiral, but now the thrust vector is directed in an opposite way so that deacceleration occurs. The Lunar spiral descends to 100 km altitude and takes about 150 days. Lunar capture orbits suitable for the Lunar GAS mission are constructed in Section 2. As seen in this section, they have an interesting behavior, and the Lagrange point, L_1, plays a role in their dynamics. The spiral orbits are described in Section 3.

In Section 4, the application of the above method towards the construction of capture orbits to other bodies such as asteroids, Mars, Jupiter, etc. is discussed.

2. Lunar Capture Orbits

Lunar capture orbits are described in this section, and an example of one which is applicable to the Lunar GAS mission is analyzed. The notation and terminology used above will be used throughout the remainder of this paper.

In order to construct a capture orbit, the location of Q must be precisely determined, or more generally the stability boundary SB must be determined. The precise definition of SB and its determination is given in the Appendix. A possible justification of its existence based on results in dynamical systems is given there. It is also seen in the Appendix that SB should not be viewed as existing in the three-dimensional position space about the Moon, but rather in the six-dimensional position-velocity space.

To determine Q, a desired inclination, latitude and longitude for the capture orbit is selected at the instantaneous moment of capture. Let L represent the radial line from the center of the Moon, each point of which has the given latitude and longitude. Assuming an approach direction for the capture orbit, we locate the critical point along L where gravitational fields of the Earth and Moon approximately balance as follows - starting at a sufficiently low Lunar altitude, propagate an orbit with an initial position on L in the given approach direction with circular velocity magnitude, until it returns to a transversal reference plane through L (See Figure 3). The Lunar relative

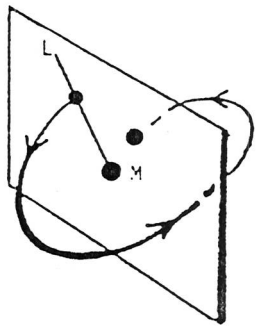

Figure 3.

eccentricity and deviation distance from the initial point when it returns to this plane is measured. For low Lunar altitude, this eccentricity and deviation distance will be near zero since the Earth's gravitational field will be felt to a small degree. Repeating this at higher initial altitudes, an altitude will be eventually reached where the eccentricity, e, will become greater than 1 after one cycle. The altitude where e = 1 gives the location of Q.

Thus, targeting to Q with the above conditions will achieve a capture orbit with a given inclination. In practice one can target to an altitude where e is slightly less than 1. This will yield a capture orbit with a bit more stability as it moves about the Moon. This targeting is discussed in the Appendix where a Newton's algorithm is derived. An alternate way of constructing a capture orbit at Q is to begin with the required capture conditions, and then integrate backwards in time until a suitable position about the Earth is attained at a point P. We choose P in this case to be an osculating periapsis point. The capture orbit described below was found in this fashion. For this orbit it was desired to be captured over the north Lunar pole. This is a constraint required by the Lunar GAS mission.

The north Lunar pole capture orbit is constructed so as to approach along the Earth Moon line. This direction was chosen for convenience, although it appears to be a direction which minimizes the required altitude for capture as will be seen in the Appendix. Assuming Lunar and solar perturbations, this orbit is shown in Figure 4. In

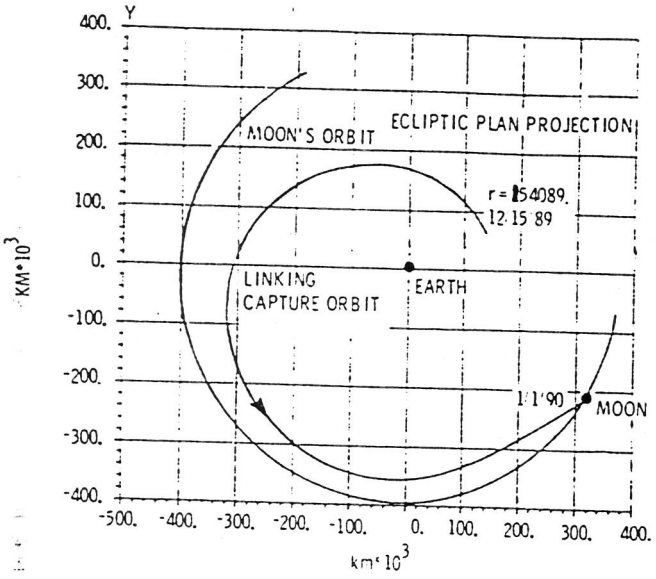

Figure 4. A Lunar Capture Orbit

this figure, which is an ecliptic plane projections, the orbit leaves P at 154,089 km from the center of the Earth on 12/15/89. Sixteen days later it approaches the capture point 35,000 km from the center of the Moon over the north Lunar pole. Its approach along the Earth Moon line at the position indicated is not seen in this inertial coordinate system. A graphic sketch of the approach geometry is seen in Figure 5. At the moment

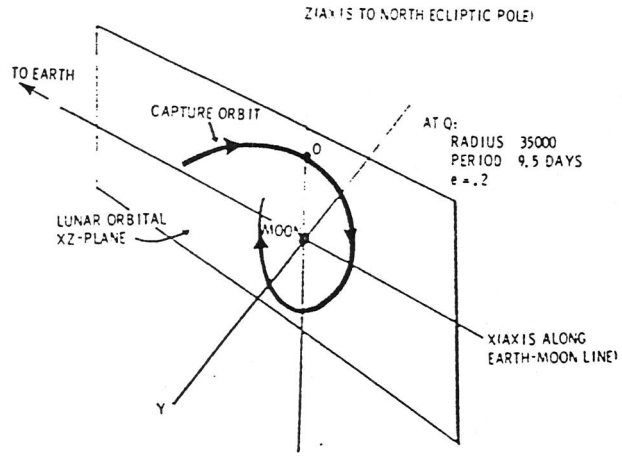

Figure 5. Approach Geometry

of capture at Q, the Lunar relative eccentricity is 0.2 with a relative Lunar period of 9.5 days.

The complex dynamics of this orbit is seen in Figure 6, 7 when it is plotted in a rotating coordinate system which rotates with the Moon of velocity of about 1 km/s, which is centered at the Earth. In this system, the Moon is fixed and it is put on the y-axis. In the ecliptic plane projection in Figure 6, the orbit moves towards the Earth Moon L_1 Lagrange point, has a closest approach to this point of about 5000 km where it moves away, forms a loop, and then approaches capture conditions at Q along the Earth Moon line. Although it

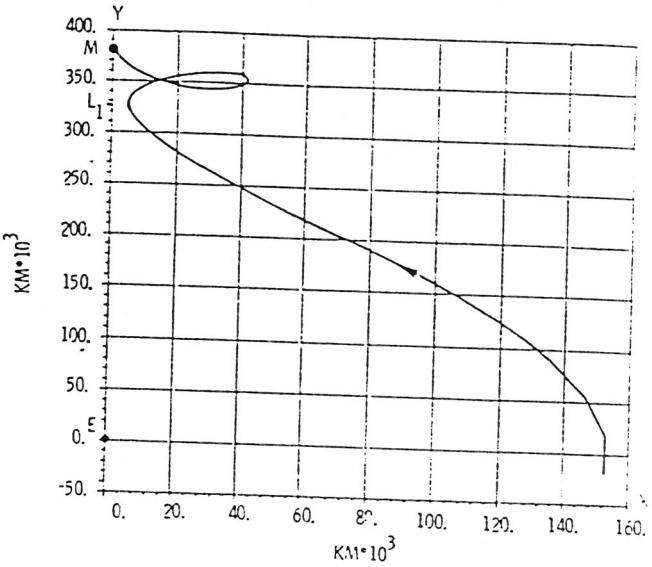

Figure 6. Capture Orbit in Rotating Coordinates

might appear at first that this motion is an artifact of being in a rotating coordinate system, this is seen not to be the case in Figure 7. The orbit executes a large out of plane motion where it rises up and then falls below the L_1 point, where it then abruptly moves up above the Earth Moon line to the point Q on the stability boundary at 35,000 km. As

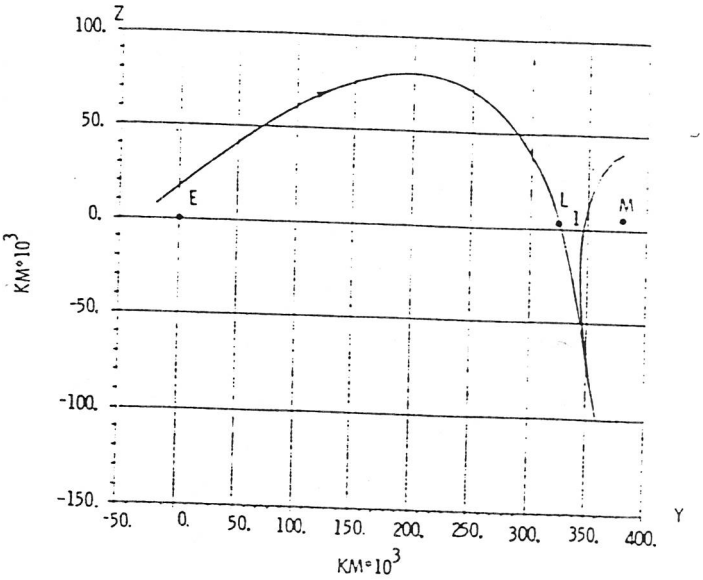

Figure 7. Out of Plane View of Capture Orbit

indicated by an argument in the Appendix, this transfer orbit is chaotic; that is, very small changes in the initial conditions at P will lead to large changes in the final position due to its behavior as it moves below the Lagrange point, and then back up above the north Lunar pole. In fact, it is seen that very small changes in the conditions at P can cause the orbit to completely avoid capture conditions. Thus, under real conditions where the required initial conditions at P will not be exactly met, orbit correction maneuvers will have to be implemented.

A reason the orbit approaches L_1 is to slow itself down in order to be reoriented to achieve Lunar polar capture conditions. Both the hyperbolic and elliptic qualities of L_1 achieve this. It is well known that of the six eigenvalues associated to the solutions of the linearized differential equations of motion at L_1, 4 are elliptic and 2 are hyperbolic. The elliptic ones are related to the well known families of halo orbits about L_1 [4,10]. This cyclic motion tends to trap the orbit as it moves near L_1. The hyperbolic character of L_1 gives an element of instability to the motion. These properties contribute to the type of motion observed in Figure 7. In addition to the linearized character of motion about L_1, the nonlinear effect of perturbations of both the Earth and Moon will cause the motion near L_1 to be complex. These issues are not pursued further in this paper.

All numerical integrations for the capture orbits were performed on a UNIVAC 1108 computer. The ephemeris of both the Earth and Moon are modeled. In practice, if a S/C were to move on such a trajectory, thrusting would be used to modify this orbit to facilitate achieving capture conditions.

The above orbit makes no assumptions on thrust profiles since none are used. Thus, it is directly applicable to the Lunar GAS mission.

In the next section we describe the spiral orbits associated with the Lunar GAS S/C as it spirals out from the Earth to P and spirals in towards the Moon from Q.

3. Earth and Moon Spiral Orbits

The method of thrusting for the Lunar GAS S/C is described in the introduction with regard to spiral orbit propagation. In this section, we describe the methods of their generation, and their properties. We begin with a discussion of the Earth spirals.

Earth Spiral

One method of generating the spiral orbits is to approximate the continuous thrusting along the 90° arcs with an equivalent impulsive $\Delta\vec{V}$ by an averaging method. The $\Delta\vec{V}$ is applied at the point a, tangential to the arc and is directed towards the Sun. This is shown in Figure 2. If applied at b, it would be directed in the anti-Sun direction. The $\Delta\vec{V}$ is estimated by averaging the tangential component of the thrust vector along the arc, assuming it is circular and then by using the rocket equation. This $\Delta\vec{V}$ is vectorially added to the circular velocity at a, and the orbit is propagated over 1/2 of a period to the point b. At b, an equivalent $\Delta\vec{V}$ is calculated and this process is repeated. The spiral orbits gradually increase their radial distance from the Earth by this process. In this model, drag is modeled which has an effect near the initial altitude of 300 km, and is about 1/2 of the thrust level. Degradation of the solar cells due to radiation in the radiation belts, roughly between 8000 - 18000 km, is modeled by a suitable reduction of the thrust level. The oblateness of the Earth, and perturbations due to the Moon and Sun are not modeled. This relatively simple model gives accurate results when compared to a more accurate one described next. In fact, the rate of spiral radial increase is nearly the same. A comparison of the results obtained by these two models is not carried out in this paper for brevity.

A more accurate model is made by modeling the continuous application of the thrust vector along the 90° arcs. This is easily done by adding the constant acceleration due to this thrust to the differential equations describing the motion of the S/C about the Earth. This model is made more precise by including the oblateness of the Earth and the perturbations due to the Moon and Sun. In addition, the Sun is tracked so that the thrust direction is oriented towards or away from the Sun direction as described in the introduction. Although thrusting occurs over 90° arcs, this is not necessary as other angles can be chosen, but it appears that 90° yields both acceptable flight times and fuel consumption.

The evolution of an example Earth spiral orbit obtained from the latter spiral model is now described. We assume an initial altitude of 300 km with circular initial conditions. An initial inclination with respect to the Earth's equator of 28.4° is assumed. The initial mass of the S/C is 145 kg and the thrust is .031 N with a constant mass flow rate of 9.59×10^{-9} kg/s. Although the thrust level should be reduced to model its degradation in the radiation belts, we hold it fixed here. Also, Earth occultations where the S/C cannot thrust are not modeled which, in fact, give a negligible effect. The variation of the radius as function of time is shown in Figure 8.

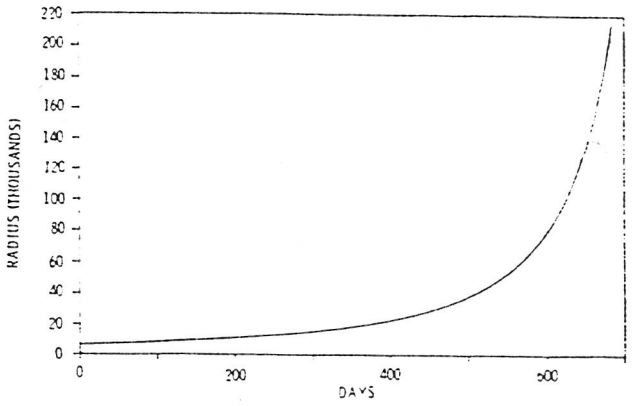

Figure 8. Radius Variation

The eccentricity of the nearly circular spiral orbits is not plotted since it stays less than .04 out to 200,000 km. The inclination with respect to the Earth's ecliptic stays nearly constant out this distance also. As seen, it takes about 670 days to spiral out to 200,000 km. Approximately 3400 individual spirals are generated, and 28 kg of propellant is used.

The variation of the node due to first order oblateness perturbations is shown in Figure 9 which yields the variation of the inclination with respect to the ecliptic in Figure 10. The variation of the node in this case is covered in (12). This is important for several reasons. In (12) Penzo shows, in particular, that the regression of the node along the Earth spiral is about 7 degrees per day in low Earth orbit which becomes negligible after about one year of spiriling as the radial distance increases. This implies that an initial value of the node should be chosen so that the node value converges to a desired one after one year. This, in turn, specifies the ecliptic inclination that the orbit converges to as it spirals away from the Earth. The oscillation of the inclination due

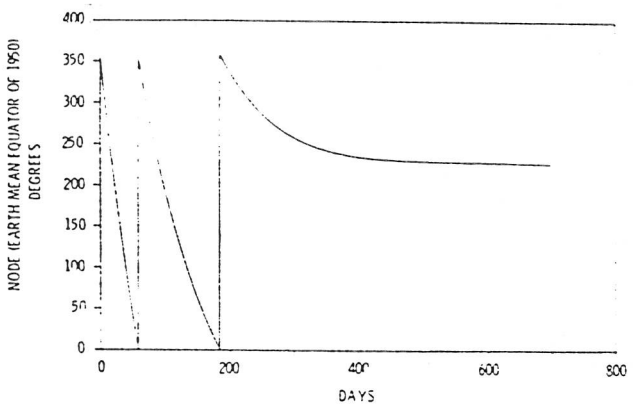

Figure 9. Nodal Variation

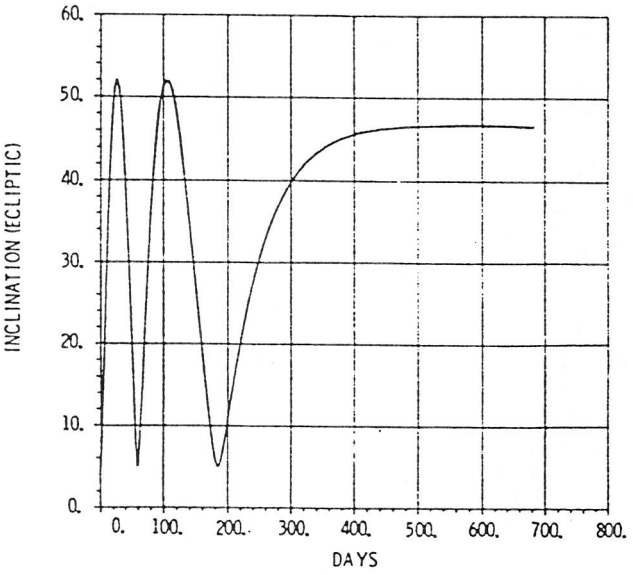

Figure 10. Ecliptic Inclination Variation

to the nodal regression is also important since the angle of the Sun on the solar panels will change, thus causing a variation in the power. The angle of the thrust vector from the orbit plane will also change causing a variation in the effect of the thrust.

Lunar Spiral

When the Earth spiral reaches the critical distance at P, the capture orbit starting at P brings the S/C to the position Q above the north Lunar pole. We assume the capture orbit described in Section 2 so that P is at a radial distance from the Earth of 154,089 km, and Q is at a radial distance of 35,000 km from the Moon. The Lunar spiral here is modeled with the averaged model described above. The equivalent ΔV approximating each thrust arc is then applied opposite to the direction of motion. Earth and Sun perturbations are not modeled, nor is the oblateness of the Moon. While the S/C is spiraling down to an altitude of 100 km, the Earth-Sun-Moon geometry is changing. The angle that the Sun direction makes on the solar panels may be small enough so that not enough power can be produced for the S/C thrusters, or the S/C may be occulted by the Moon. We ignore these effects here for brevity. The initial mass of the S/C at Q is 118.5 kg and the thrust is 0.031N. To descend to a 100 km altitude, it takes 121 days and 5 kg of fuel is used.

Performance

The variation of the total time of flight from the initial Earth altitude of 300 km to the final Lunar altitude at 100 km and fuel consumption as a function of initial mass is now described. We look at the three initial masses of 125, 145, 170 kg. The Earth and Lunar spirals are generated as described above using the latter and former spiral models respectively. However, we also model the degradation of the solar cells by reducing the thrust F as follows: For 0-150 days, F = .0424N, and for 150 days until the end of the Lunar spiral at 100 km altitude, F = .031 N. We also assume the capture orbit described in Section 2 so that the final position P of the Earth spiral and the beginning position Q of the Lunar spiral are the same as above. It is remarked when the Earth spiral reaches P, the orbital elements of the spiral must match the required conditions for the capture orbit which requires e = .3, and the spiral orbit must also reach P with the correct Earth-Sun-Moon geometry. This problem is briefly discussed after the performance data is presented. In Tables 1,2 the variation of the time of flight TF in days and fuel consumption DM in kg is given as a function of the initial mass M_o. The variation of TF and DM are graphed in Figure 11.

Transition

A necessary problem to solve is to insure that the spiral orbit actually reaches the position P with (1) the Sun in a suitable position in order to

M_o	TF - Earth Spiral	Capture Orbit	Lunar Spiral	Total TF
125	545	16	94	655
145	633	16	121	770
170	752	16	140	908

Table 1. Time of Flight Variation

M_o	DM - Earth Spiral	Capture Orbit	Lunar Spiral	Total DM
125	22.7	0	3.9	26.6
145	26.5	0	5.0	31.5
170	31.3	0	5.8	37.1

Table 2. Fuel Consumption Variation

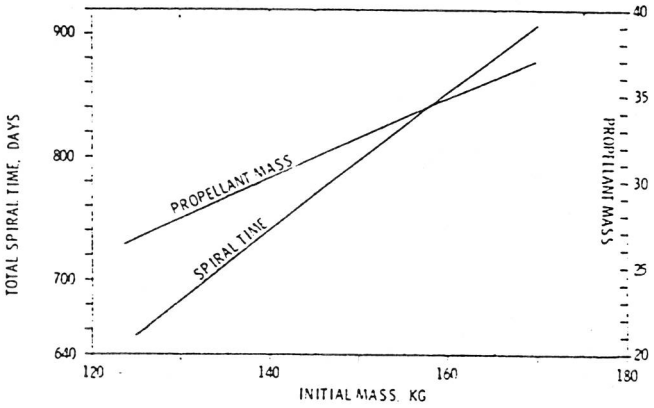

Figure 11. Performance Curves

power the solar cells, and (2) the osculating orbital elements of the spiral at P match those of the capture orbit. Both of these conditions can be satisfied by using a Newton's targeting algorithm, i.e. a differential correction algorithm, which varies the duration and direction of the thrust arcs prior to arriving at P with the required velocity vector. This is not described here since it is similar to the type of algorithm described in the Appendix for the Lunar capture orbit targeting. For the sake of simplicity of argument, we assume that the spiral arrives at P with the correct velocity direction. In general the magnitude of the velocity will not match that of the capture orbit. This manifests itself in the nonequality of the eccentricities. Typically, an Earth spiral at P has an eccentricity of approximately .02. But the capture orbit has an eccentricity of .3. The eccentricity of the spiral at P can be increased to 0.3 by doing a succession of spiral orbits by only thrusting on one side of the spiral, where the center of the thrust arc lies at the point P. Approximately 8 of these spirals are required to increase the eccentricity. This increases the flight time to about 70 days. This increase in flight time is not factored into the above performance data. The most efficient way of achieving the correct conditions at P is to apply the Newton's method to determine a suitable thrusting variation.

4. Applications to Other Capture Orbits

Capture orbits to other bodies can be constructed in a way similar to those in Section 2. The size of the stability boundary about a body M_1 depends on the degree of the perturbations of other bodies. We assume for the sake of argument that there is only one other perturbing body M_2, and that the mass of particle m to be captured by M_1 is negligible with respect to the masses of M_1 and M_2. One can take, e.g., M_1 = Moon and M_2 = Earth as was done in this paper. On the other hand, there are many other possibilities. For example, if M_2 = Sun, then M_1 could be chosen to be an asteroid, comet or Mars, etc. The collinear Lagrange point L_1 between M_1 and M_2 will play a role in the dynamics of capture orbits from M_2. The particle m need not be a S/C. Thus, it is conceivable that Phobos or Diemos could have been captured by Mars by such orbits. Similarly, some of the satellites of Jupiter, as well as those of the other outer planets, could have been captured. For this to be the case, these satellites must have not only been simply captured, but captured in such a way that the motion about M_1 is stable. These conditions are difficult to achieve, but the chances of achieving them were probably much higher at the early stages of the solar system formation due to a possible large number of objects moving throughout the solar system.

5. Appendix

This section is subdivided into two topics referred to in the previous sections. The first topic describes the stability domain SB in more detail than above. An argument is also given which gives a possible justification for its existence. The other topic describes a Newton's algorithm which will allow targeting to Lunar capture conditions. Possible difficulties in implementing this algorithm are briefly discussed.

The Stability Boundary and Its Estimation

The stability boundary was heuristically described in the introduction. SB is estimated by carrying out a procedure described in the beginning of Section 2 to determine the location about the Moon of the point Q that would be necessary in order to achieve a capture conditions. In this case, a critical position on the radial line L shown in Figure 3, which has the given latitude, ψ and longitude, θ, with respect to the Moon, is determined where gravitational effects of the Earth and Moon balance. This position on L was determined by propagating orbits from L with circular initial conditions and monitoring their final state after approximately one cycle on a reference plane. This plane is called a Poincare section [3]. These orbits along L are all propagated with the required inclination of the capture orbit, and with a given approach direction from the Earth. Monitoring, for example, the eccentricity, the location of the critical point Q is the position on L where after one cycle, e goes from an initial value of zero to one.

For given ψ and θ, the radial distance from the Moon where the gravitational fields balance depends on the approach direction. For a fixed ψ,θ, there is 1 parameter family of possible approach directions and therefore also of corresponding possible critical radial distances. The set of approach directions over the north Lunar pole is shown in Figure 12. This set of approach directions, V, and radial distances, r, is two-dimensional. We call this set

$$U(\psi,\theta) = (\vec{V}(\psi,\theta),\ r(\psi,\theta)) \quad .$$

The vectors $\vec{V}$ are constrained to two-dimensional planes perpendicular to the respective radial vectors from the Moon. This set defines a two-dimensional slice of SB for the given ψ,θ. If ψ,θ are allowed to also vary where $-90 \leq \psi \leq 90$, $0 \leq \theta < 360$, then they make a two dimensional set, Q. This set together with the corresponding two-dimensional sets U make a four-dimensional set which is defined to be SB. Thus,

$$SB = \bigcup_{\psi,\theta \in Q} U(\psi,\theta) \quad .$$

It is remarked that since SB depends on the approach directions, then it exists in position and velocity space, or phase space, which has six dimensions. SB can be viewed as a 4-dimensional region existing in the 6-dimensional phase space.

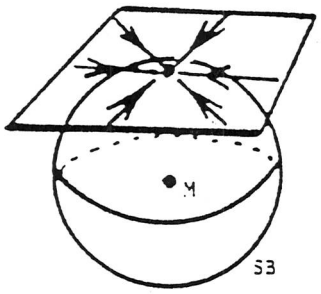

Figure 12. Approach Directions

SB can be numerically estimated by choosing a given ψ,θ and then determining the critical radii along four basic approach directions. For example, over the north Lunar pole, $\psi = 90$ and θ is arbitrarily fixed, e.g. to 0, and the approach directions chosen are labeled 1,2,3,4, on the plane as shown in Figure 13. We first focus on the direction a_1, and monitor e at the end of one circular period where initially $e = 0$. The direction a_1 is in the anti-Earth direction. The initial radial distance is r_o and the final is r_F. The results are shown in Table 3. The initial time of propagation is fixed at 1/1/1990 .

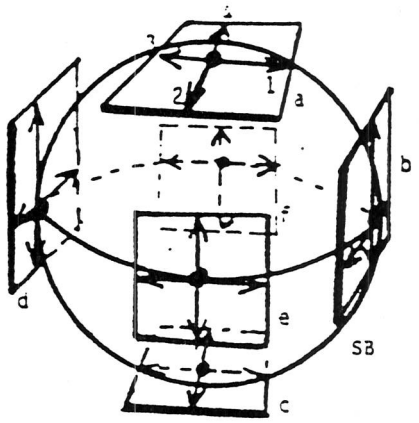

Figure 13. Estimation of SB

r_o	r_F	e (Final)
32,500	21,757	.39
37,500	24,019	.51
40,000	47,901	.42
42,500	76,753	1.11
45,000	113,305	3.05
50,000	200,610	11.76

Table 3. Variation of the Eccentricity

From Table 3 we conclude that the critical radius is approximately 42,000 km. For the other directions we find that $a_2 = 68{,}000$, $a_3 = 40{,}000$, $a_4 = 46{,}000$.

Similar results are obtained for the other locations b, c, d, e, f shown in Figure 13, but are not described for brevity.

It is remarked that topologically SB is equivalent to the cartesian product of a two-dimensional sphere, S^2, and a two-dimensional cylinder, C^2. Thus,

$$SB \simeq S^2 \times C^2 \quad .$$

Existence of SB (Optional)

A brief argument is given to motivate the existence of SB. It is assumed for the sake of argument that the eccentricity of the Moon's orbit is zero, and that after capture, the orbit remains on a fixed plane E of motion corresponding to the instantaneous planar motion at the moment of capture. These erroneous assumptions will be relaxed later. On the plane of motion, it can be shown that the motion can be described by a two-dimensional transformation of a type which is area preserving.(1) For these transformations, it can

be shown that nearly circular motion starting sufficiently near the Moon and constrained to E will be quasi-periodic and stable for all time. This follows by an application of the Kolmogorov-Arnold-Moser theorem.[1] But this type of motion cannot persist at arbitrarily large distances from the Moon. General results by J. Mather[9] on area preserving transformations when applied to the motion on E shows that there exists a critical distance r^* from the Moon where quasi-periodic motion, in general, will breakdown. It is not possible to relate r^* to the critical distances described above where circular motion goes from elliptic to hyperbolic after one cycle about the Moon. This is because in the more general setting where the Moon's eccentricity is not zero, and the motion need not be constrained to E, Mather's results cannot be applied. However, it is possible that a more general theorem exists which will predict the breakdown of quasi-periodic motion about the Moon in the general setting. The numerical results presented here tend to point in this direction. If this were the case, then the distances from the Moon where quasi-periodic will break down may be related to the critical distances measured above for an orbit with a given inclination, i, and ψ, θ which goes from elliptic to hyperbolic states after one cycle. It is numerically observed, in general, that the motion often occuring when the quasi-periodic breaks down is chaotic.[5]

A Newton's Method For Targeting to Capture Conditions

We describe an algorithm which will allow targeting to Lunar capture conditions at Q near the Moon from a position P about the Earth. It is assumed that the critical distance above the Moon has been determined from $\vec{V}$, ψ, θ for capture. Thus, the position coordinates (q_1,q_2,q_3) of Q are determined. The required velocity coordinates $(\dot{q}_1,\dot{q}_2,\dot{q}_3)$ at Q are also determined by knowing the approach direction. This velocity vector is assumed to be perpendicular to the position vector to Q. The magnitude of the velocity has the value of the magnitude of circular velocity at the given radial distance. We set

$$b = (q_1,q_2,q_3,\dot{q}_1,\dot{q}_2,\dot{q}_3) \quad .$$

Thus, b is a vector of six components. We delete the vector notation, $\underline{b}$, for simplicity.

Thus, given b, we would like to determine both the position (p_1,p_2,p_3) of P and the velocity, $(\dot{p}_1,\dot{p}_2,\dot{p}_3)$, required to achieve a capture orbit which arrives at Q a time T later to be determined. We set

$$a = (p_1,p_2,p_3,\dot{p}_1,\dot{p}_2,\dot{p}_3) \quad .$$

We would like to determine a and T from an initial guess a_o. If we let f represent the association of a_o to b_1 on a reference plane by the propagation of the trajectory, then

$$b_1 = f(a_o) \quad . \qquad (1)$$

The time of propagation is given by T_1. In general $b_1 \neq b$ and $T_1 \neq T$ since $a_o \neq a$, where a is the desired solution. Thus, we want to solve the boundary value problem for a. (See Figure 14).

$$f(a) = b \quad . \qquad (2)$$

Expanding (2) in a Taylor series about $a = a_o$ yields

$$f(a) = f(a_o) + \frac{\partial f}{\partial a}(a_o)(a-a_o) + \ldots = b \qquad (3)$$

where

$$\Omega = \frac{\partial f}{\partial a}(a_o)$$

is defined to be the 6x6 variational matrix. In component form, an element λ_{ij} of this matrix is given by

$$\lambda_{ij} = \frac{\partial f_i}{\partial a_j}(a_o)$$

where i,j = 1,2,...6.

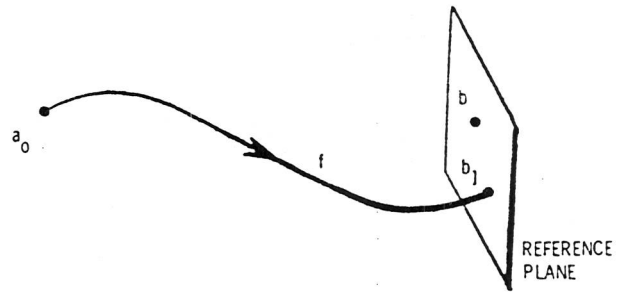

Figure 14. Newton's Iteration

Truncating quadratic and higher order terms in (3) to approximate (2) implies initially from (1) that

$$a_1 = \Omega^{-1}(a_o)(b-b_1) + a_o$$

provided Ω is nonsingular. a_1 should yield a better guess; that is, $b_2 = f(a_1)$ should lie closer in distance to b. Iterating,

$$b_{n+1} = f(a_n) \qquad (4a)$$

where

$$a_{n+1} = \Omega^{-1}(a_n)(b-b_{n+1}) + a_n, \qquad (4b)$$

$n = 1,2,3,\ldots$ If $|a-a_o| = \sqrt{\sum_{k=1}^{6} (a_k - a_{ok})^2}$

is sufficently small, then (4a,b) converges,

$$b_n \longrightarrow b$$
$$a_n \longrightarrow a$$

as follows from (6). Moreover, $T_n \longrightarrow T$.

From the sensitive behavior of the capture orbit shown in Figure 7 as a function of initial conditions, it is seen that the computation of $\Omega^{-1}(a_k)$, $k = 1,2,\ldots$ may be difficult. An accurate difference scheme should be used to compute the elements of Ω.

Summary

The existence of Lunar capture orbits is numerically demonstrated, and they are used to successfully construct a trajectory from the Earth to the Moon for the Lunar GAS mission. These capture orbits are ballistic and can be used for other missions which may or may not require low thrust. Ideas from dynamical systems theory are used to motivate the existence of capture orbits and the concept of 'stability boundary'. The use of ballistic capture orbits represents a different approach to mission design.

Acknowledgements

I am grateful to K. Nock for many valuable suggestions which has helped the progress of the orbit analysis, and to N. Lin for her help on the computer graphics. I would also like to thank D. Byrnes, R. Diehl, J. Kwok, F. Nicholson and P. Penzo at JPL, and A. Katok and S. Wiggins at Caltech for many helpful suggestions and discussions.

The research described in this paper was carried out at the Jet Propulsion Laboratory, California Institute of Technology, under a contract with the National Aeronautics and Space Administration.

References

1. Arnold, V. I., Mathematical Methods of Classical Mechanics, Springer Verlag, 1978.

2. Arnold, V. I.; Avez, A., Ergodic Problems of Classical Mechanics, Benjamin, Inc., 1968.

3. Belbruno, E. A., "A New Regularization of the Restricted-Three-Body Problem With An Application", Celest. Mech, V25, pp 397-415, 1981.

4. Gomez, G.; Llibre, J.; Martinez, R.; Simo, C., Station Keeping of Libration Point Orbits, ESOC Final Report: Executive Summary, Barcelona, Spain, Nov. 1985.

5. Greene, J. M., "The Calculation of KAM Surfaces", Nonlinear Dynamics, Edited by R. Helleman, Annals of New York Academy of Sciences, V357, pp 80-89, 1980.

6. Isaacson, E.; Keller, H., Analysis of Numerical Methods, Wiley & Sons, 1966.

7. Katok, A., "Some Remarks On Birkhoff and Mather Twist Map Theorems", Ergodic Theory and Dynamical Systems, 2, 1982.

8. Kwok, J., "The Artificial Satellite Analysis Program (ASAP)", JPL EM 312/85-140, 1985.

9. Mather, J., "Non-existence of Invariant Circles", Journal of Topology, 1983.

10. Nicholson, F. T., "Effect of Solar Perturbations on Motion Near the Collinear Earth-Moon Libration Points", AIAA Journal, V5, No. 12, 1967.

11. Nock, K.; Aston, G.; Stella, P. M.; Salazar, R. P., "Lunar Getaway-Special (GAS) Spacecraft", AIAA Paper 87-1051, 19th AIAA/DGLR/JSASS International Electric Propulsion Conference, Colorado Springs, 1987.

12. Penzo, P., "Nodal Regression Effect on Low Thrust Spiral Trajectories", Internal JPL IOM 312/87.1-51-PAP, March 1987.

13. Szebehely, V., Theory of Orbits, Academic Press, 1967.